

Calculation of quantum correlation spectra using the regression theorem

Wang Kaige¹, A. Sinatra^{2,a}, and L.A. Lugiato³

¹ CCAST (World Laboratory), P.O. Box 8730, Beijing 100080, P.R. China
and

Department of Physics, Beijing Normal University, Beijing 100875, P.R. China

² Laboratoire Kastler Brossel, École Normale Supérieure, 75231 Paris, France

³ INFN, Dipartimento di Scienze Chimiche, Fisiche e Matematiche, Università dell' Insubria, 20100 Como, Italy

Received 30 August 1999 and Received in final form 4 July 2000

Abstract. We present a simple method, based on the quantum regression theorem, to calculate the quantum correlation spectra for two optical beams in the linearized fluctuation regime. As an application, we discuss the dynamical instability, the squeezing spectra and the QND properties of a crossed Kerr-type dispersive model.

PACS. 42.50.Dv Nonclassical field states; squeezed, antibunched, and sub-Poissonian states; operational definitions of the phase of the field; phase measurements – 42.50.Lc Quantum fluctuations, quantum noise, and quantum jumps – 42.65.Pc Optical bistability, multistability, and switching

1 Introduction

Both dynamical and quantum features of non linear optical systems are widely studied in quantum optics. Among the quantum features, the quantum correlations of the optical field that can be engineered in properly designed experiments, represent an important issue which may find practical applications in optical communications and high precision measurements.

The first theoretical proposals to manipulate electromagnetic field correlations at the quantum level appeared in the seventies and in the early eighties in the context of the production of squeezed states of light (see *e.g.* [1,2] for a review). Since the first proposals, the important role of two photon processes in the production of squeezed states was pointed out [3,4], as well as the important role played by an optical cavity which would enhance the non-linear two-photon process [5,6]. Many different schemes were then readily put forward to produce efficiently squeezing by using non linear media in optical cavities such as $\chi^{(2)}$ crystals displaying parametric amplification or second harmonic generation [7], as well as two or three level atoms displaying a Kerr non linearity [8–10], and optical bistability [11–13]. Soon after, non linear optical systems have been considered as candidates for Quantum Non Demolition (QND) measurement schemes [14–18], stimulating a rapid development of the field both on theoretical and experimental ground [19–37].

In a QND experiment a quantum measurement is performed on the system in such a way that the noise introduced by the measurement does not couple back to the measured observable. In optics, a QND measurement of the quantum fluctuations of a propagating light beam can be performed by coupling the beam, usually called “signal”, to a second beam called “meter”. The coupling can be supplied by a nonlinear medium and it should be designed in such a way that a direct measurement performed on the meter allows to obtain information on the signal quantum fluctuations without changing them, or in a “non demolition” way.

The effectiveness of a QND measurement can be evaluated by three criteria [20,21], which are normalized quantum correlations between the input and the output fields fluctuations. In order to calculate such correlations a linearized treatment of quantum fluctuations is usually performed. The linearization techniques make a complicated nonlinear system solvable and are extensively applied when the quantum fluctuations are much smaller than the stationary working values. An example in quantum optics is the semiclassical linear input-output theory which was developed for computing the quantum fluctuations in one-photon [38,39] and two-photon processes [19,40]. Linear response techniques were also generalized for evaluating the quantum correlation spectra for QND measurements [23,41,42]. Nevertheless it seems to us that a detailed and handy article explaining how to calculate the quantum correlations between the input and output fields which characterize a QND measurement is still missing in the literature.

^a e-mail: alice.sinatra@lkb.ens.fr

In this paper we derive the useful formulae of the quantum correlation spectra for a QND measurement in the linearized regime using the quantum regression theorem. The advantage of the presented method is that it is quite simple and it allows a straight forward numerical implementation. The method is general and it can be applied to the case in which the atomic internal degrees of freedom, and the spontaneous emission of the atoms are explicitly taken into account (see *e.g.* [37]).

As an example, we apply our method to a model describing a crossed Kerr-type dispersive nonlinearity which provides a favorable QND coupling scheme between two optical beams. The Kerr-type dispersive model has been extensively studied in previous works [18–20, 29, 43]; despite its simplicity it catches the interesting physics and it is a useful tool to understand real systems.

We study here the Kerr model analytically in the general case for the system parameters; and we complete the analysis performed in [29] by pointing out simple relations among the dynamical instability in the Kerr model, the reduction or enhancement of quantum noise in the output fields and the QND effectiveness of the system.

2 QND criteria and squeezing spectra

We consider the case in which two beams, initially a coherent state, pass through an optical device made by a cavity filled by a nonlinear medium. Inside the cavity the two fields are described by the bosonic operators a_j and a_j^\dagger with $j = 1, 2$ which verify

$$[a_i, a_j] = 0, \quad [a_i^\dagger, a_j^\dagger] = 0, \quad [a_i, a_j^\dagger] = \delta_{ij} \quad (i, j = 1, 2), \quad (1)$$

and commute with the other system operators. The intracavity system dynamics is described by a master equation (ME)

$$\frac{d\rho}{dt} = \frac{1}{i\hbar}[H, \rho] + \Lambda, \quad (2)$$

where H is the Hamiltonian of the system and Λ describes irreversible part of the dynamics. In general, the dynamics includes both field variables (associated with the operators a_i, a_i^\dagger) and atomic variables. In the Linblad form

$$\Lambda = \sum_j \frac{\kappa_j}{2} ([c_j, \rho c_j^\dagger] + [c_j \rho, c_j^\dagger]), \quad (3)$$

where the sum is over all the system operators c_j coupled to the reservoir. In models that include only field variables, $c_j = a_j$, ($j = 1, 2$) and κ_j are the decay constants of the fields inside the cavity [44].

We assume that the beams are initially in a coherent state. As the beams pass through the device, their quantum noise properties are changed and correlations between the beams can be established. Properly defined correlation coefficients characterize the efficiency of the device to reduce the quantum fluctuations in some quadrature of the

outgoing fields, or to perform quantum non demolition measurements of one field fluctuations.

In the frequency domain, one defines the correlation coefficient $C^2(p, q)$ between two Hermitian operators p and q as:

$$C^2(p, q) \equiv \frac{|\langle pq \rangle_{\text{sym}}(\omega)|^2}{V(p)V(q)}, \quad (4)$$

$$\langle pq \rangle_{\text{sym}}(\omega) \equiv \frac{1}{2} \int_{-\infty}^{\infty} dt e^{-i\omega t} \langle p(t)q + qp(t) \rangle, \quad (5)$$

$$V(p) \equiv \int_{-\infty}^{\infty} dt e^{-i\omega t} \langle p(t)p \rangle = \langle pp \rangle_{\text{sym}}. \quad (6)$$

The quantity $V(p)$ is the squeezing spectrum of the observable p . Note that, $\langle pq \rangle_{\text{sym}}(\omega) = [\langle pq \rangle_{\text{sym}}(-\omega)]^* = \langle qp \rangle_{\text{sym}}(-\omega)$.

For us, the Hermitian operators are the *fluctuations* of the input and output fields, in a given quadrature corresponding to some given reference phases θ_j^{in} and θ_j^{out} respectively

$$x_j^{\text{in}} = \frac{1}{2}(a_j^{\text{in}} \exp[-i\theta_j^{\text{in}}] + h.c.), \\ x_j^{\text{out}} = \frac{1}{2}(a_j^{\text{out}} \exp[-i\theta_j^{\text{out}}] + h.c.). \quad (7)$$

In (7) and in the following we have redefined the operators a_j and a_j^\dagger by subtracting their steady state mean values $\langle a_j \rangle$ so that they represent fluctuations of the fields. If the beam 1 is the meter and the beam 2 the signal with respect to the QND measurement, the three correlation coefficients which are important to characterize the QND measurement are [20, 21, 25]

$$C_1^2 \equiv C^2(x_2^{\text{in}}, x_1^{\text{out}}), \quad C_2^2 \equiv C^2(x_2^{\text{in}}, x_2^{\text{out}}), \\ C_3^2 \equiv C^2(x_2^{\text{out}}, x_1^{\text{out}}). \quad (8)$$

The first two coefficients C_1^2 and C_2^2 are correlations between the output fields fluctuations of the QND device and the input fields fluctuations. They quantify the effectiveness of the measurement and its nondemolition properties respectively, and they represent the first two criteria to characterize a real QND measurement. A third criterion concerning the fluctuations of the output fields is the conditional variance $V_c(x_2^{\text{out}}|x_1^{\text{out}})$ of the signal field given the result of a measurement on the meter field. The conditional variance characterizes the quantum state preparation (QSP) properties of the system, and it is expressed as [21]

$$V_c(x_2^{\text{out}}|x_1^{\text{out}}) = V(x_2^{\text{out}})(1 - C_3^2). \quad (9)$$

To be specific, the two inequalities, $C_1^2 + C_2^2 > 1$ and $V_c < 1/4$ (shot noise level), are introduced as violation of classical limits of measurement [30, 31]. For a perfect QND measurement $C_1^2 = C_2^2 = 1$ and $V_c(x_2^{\text{out}}|x_1^{\text{out}}) = 0$.

The variances $V(x_j^{\text{out}})$ ($j = 1, 2$), or squeezing spectra, characterize the quantum fluctuations of the output fields for the selected quadrature.

3 The input and output fields correlations

The QND coefficients C_1^2 and C_2^2 involve correlations between the input and the output fields, while the coefficient C_3^2 and the squeezing spectra involve correlations between the output fields only. In order to calculate all these coefficients we need to express them in terms of intracavity operators.

Let us consider a single port optical cavity. The boundary conditions for the intracavity, input and output fields are [45]

$$a_j^{\text{out}}(t) - a_j^{\text{in}}(t) = \sqrt{2\kappa_j} a_j(t) \quad (j = 1, 2). \quad (10)$$

The commutation rules of the free fields a_j^{in} are

$$[a_j^{\text{in}}(t), a_{j'}^{\dagger\text{in}}(t')] = \delta_{jj'} \delta(t - t'), \quad (11)$$

and the same holds for a_j^{out} . If B is any system operator, the causality hypothesis imposes [45]

$$\begin{aligned} [B(t), a_j^{\text{in}}(t')] &= [B(t), a_j^{\dagger\text{in}}(t')] = 0 \quad \text{for } t' > t \\ [B(t), a_j^{\text{out}}(t')] &= [B(t), a_j^{\dagger\text{out}}(t')] = 0 \quad \text{for } t' < t \end{aligned} \quad (j = 1, 2), \quad (12)$$

therefore, by using (10),

$$\begin{aligned} [B(t), a_j^{\text{in}}(t')] &= -u(t - t') \sqrt{2\kappa_j} [B(t), a_j(t')] \\ [B(t), a_j^{\text{out}}(t')] &= u(t' - t) \sqrt{2\kappa_j} [B(t), a_j(t')] \\ [B(t), a_j^{\dagger\text{in}}(t')] &= -u(t - t') \sqrt{2\kappa_j} [B(t), a_j^\dagger(t')] \\ [B(t), a_j^{\dagger\text{out}}(t')] &= u(t' - t) \sqrt{2\kappa_j} [B(t), a_j^\dagger(t')] \end{aligned} \quad (j = 1, 2), \quad (13)$$

where $u(t)$ is the step function

$$u(t) = \begin{cases} 1 & t > 0 \\ 0 & t < 0 \end{cases}. \quad (14)$$

We consider the case in which the input fields are in a coherent state. With the help of equations (10–13), one can readily derive the input-output and output-output correlations expressed in terms of intracavity correlations

$$\begin{aligned} \langle a_i^{\text{out}}(t) a_j^{\text{in}} \rangle &= \langle a_i^{\dagger\text{in}}(t) a_j^{\dagger\text{out}} \rangle = 0 \\ \langle a_i^{\dagger\text{out}}(t) a_j^{\dagger\text{in}} \rangle &= -2\sqrt{\kappa_i \kappa_j} u(t) \langle [a_i^\dagger(t), a_j^\dagger] \rangle \\ \langle a_i^{\text{in}}(t) a_j^{\text{out}} \rangle &= -2\sqrt{\kappa_i \kappa_j} u(-t) \langle [a_i(t), a_j] \rangle \\ \langle a_i^{\dagger\text{out}}(t) a_j^{\text{in}} \rangle &= \langle a_i^{\dagger\text{in}}(t) a_j^{\text{out}} \rangle = 0 \\ \langle a_i^{\text{out}}(t) a_j^{\dagger\text{in}} \rangle &= -2\sqrt{\kappa_i \kappa_j} u(t) \langle [a_i(t), a_j^\dagger] \rangle + \delta_{ij} \delta(t) \\ \langle a_i^{\text{in}}(t) a_j^{\dagger\text{out}} \rangle &= -2\sqrt{\kappa_i \kappa_j} u(-t) \langle [a_i(t), a_j^\dagger] \rangle + \delta_{ij} \delta(t) \end{aligned} \quad (i, j = 1, 2), \quad (15)$$

$$\begin{aligned} \langle a_i^{\text{out}}(t) a_j^{\text{out}} \rangle &= 2\sqrt{\kappa_i \kappa_j} \{ u(t) \langle a_i(t) a_j \rangle + u(-t) \langle a_j a_i(t) \rangle \} \\ \langle a_i^{\dagger\text{out}}(t) a_j^{\dagger\text{out}} \rangle &= 2\sqrt{\kappa_i \kappa_j} \{ u(-t) \langle a_i^\dagger(t) a_j^\dagger \rangle + u(t) \langle a_j^\dagger a_i^\dagger(t) \rangle \} \\ \langle a_i^{\dagger\text{out}}(t) a_j^{\text{out}} \rangle &= 2\sqrt{\kappa_i \kappa_j} \langle a_i^\dagger(t) a_j \rangle \\ \langle a_i^{\text{out}}(t) a_j^{\dagger\text{out}} \rangle &= 2\sqrt{\kappa_i \kappa_j} \langle a_j^\dagger a_i(t) \rangle + \delta_{ij} \delta(t) \end{aligned} \quad (i, j = 1, 2). \quad (16)$$

4 Reformulation of the QND criteria and squeezing spectra

Equations (15, 16) allow us to express the QND coefficients defined in section 2 terms of “response functions” of the form

$$R_{ij} = \int_0^\infty \langle [\beta_i(t), \beta_j] \rangle e^{-i\omega t} dt, \quad (17)$$

and correlation functions of the form

$$S_{ij} = \int_{-\infty}^\infty \langle \langle :: \beta_i(t) \beta_j :: \rangle \rangle e^{-i\omega t} dt, \quad (18)$$

where the variables $(\beta_1, \beta_2, \beta_3, \beta_4) \equiv (a_1^\dagger, a_1, a_2^\dagger, a_2)$ represent the fluctuations of the creation and annihilation operators of the two fields and the double dots in (18) mean time and normal ordering. In particular for the input-output correlations appearing in the QND coefficients C_1 the C_2 we find:

$$\begin{aligned} \langle x_1^{\text{out}} x_2^{\text{in}} \rangle_{\text{sym}}(\omega) &= \\ &= -\frac{1}{4} \sqrt{\kappa_1 \kappa_2} \{ -R_{24} e^{-i(\theta_2^{\text{in}} + \theta_1^{\text{out}})} + R_{13} e^{i(\theta_2^{\text{in}} + \theta_1^{\text{out}})} \\ &\quad - R_{14} e^{-i(\theta_2^{\text{in}} - \theta_1^{\text{out}})} + R_{23} e^{i(\theta_2^{\text{in}} - \theta_1^{\text{out}})} \}, \end{aligned} \quad (19)$$

$$\begin{aligned} \langle x_2^{\text{out}} x_2^{\text{in}} \rangle_{\text{sym}}(\omega) &= \frac{1}{4} \cos(\theta_2^{\text{out}} - \theta_2^{\text{in}}) \\ &= \frac{1}{4} \kappa_2 \{ -R_{44} e^{-i(\theta_2^{\text{out}} + \theta_2^{\text{in}})} + R_{33} e^{i(\theta_2^{\text{out}} + \theta_2^{\text{in}})} \\ &\quad + R_{43} e^{-i(\theta_2^{\text{out}} - \theta_2^{\text{in}})} - R_{34} e^{i(\theta_2^{\text{out}} - \theta_2^{\text{in}})} \}. \end{aligned} \quad (20)$$

If in equations (19, 20) we set $\omega \rightarrow -\omega$, which amounts to taking the conjugate of the original correlations, the correlation coefficients do not change. Note also that the presence of the step function in equations (15, 16) leads naturally to an integral from zero to infinity as in equation (17).

The variances of the input and output fields for the considered quadratures are:

$$\begin{aligned} V(x_1^{\text{in}}) &= V(x_2^{\text{in}}) = \frac{1}{4}, \\ V(x_1^{\text{out}}, \omega) &= \frac{1}{4} + \frac{1}{2} \kappa_1 [S_{22}(\omega) \exp(-2i\theta_1^{\text{out}}) \\ &\quad + S_{11}(\omega) \exp(2i\theta_1^{\text{out}}) + S_{21}(\omega) + S_{12}(\omega)], \\ V(x_2^{\text{out}}, \omega) &= \frac{1}{4} + \frac{1}{2} \kappa_2 [S_{44}(\omega) \exp(-2i\theta_2^{\text{out}}) \\ &\quad + S_{33}(\omega) \exp(2i\theta_2^{\text{out}}) + S_{43}(\omega) + S_{34}(\omega)]. \end{aligned} \quad (21)$$

Finally, the cross correlation for C_3^2 is

$$\begin{aligned} \langle x_1^{\text{out}} x_2^{\text{out}} \rangle_{\text{sym}} &= \frac{1}{2} \sqrt{\kappa_1 \kappa_2} \{ S_{42} e^{-i(\theta_2^{\text{out}} + \theta_1^{\text{out}})} \\ &+ S_{31} e^{i(\theta_2^{\text{out}} + \theta_1^{\text{out}})} + S_{41} e^{-i(\theta_2^{\text{out}} - \theta_1^{\text{out}})} + S_{32} e^{i(\theta_2^{\text{out}} - \theta_1^{\text{out}})} \}. \end{aligned} \quad (22)$$

Equations (19–22) can then be used to express the QND coefficients and the squeezing spectra in terms of the response and correlation matrix R and S .

5 Correlations and response functions

5.1 Use of the quantum regression theorem

Let $\{\xi_i\} = \beta_1, \beta_2, \beta_3, \beta_4, \dots$, ($i = 1 \dots n$) be set of the quantum fluctuations of all the system operators. In general, they include both the field operators and atomic operators; the field operators refer to the intracavity fields. In the linearized regime for quantum fluctuations we have

$$(d/dt)\langle \xi_i(t) \rangle = - \sum_j M_{ij} \langle \xi_j(t) \rangle, \quad (23)$$

where M_{ij} is the drift matrix. According to the quantum regression theorem [46], for $t > 0$ we can write

$$\begin{aligned} (d/dt)\langle \xi_i(t) B \rangle &= - \sum_j M_{ij} \langle \xi_j(t) B \rangle \\ (d/dt)\langle B \xi_i(t) \rangle &= - \sum_j M_{ij} \langle B \xi_j(t) \rangle, \end{aligned} \quad (24)$$

where B can be any function of fluctuation operators $\{\xi_i\}$, evaluated at the time $t = 0$ *i.e.* $B = B(\{\xi_i(0)\})$. We perform the Laplace transformation to (24) and obtain:

$$\begin{aligned} \int_0^\infty \langle \xi_i(t) B \rangle e^{-pt} dt &= \sum_j (M + pI)_{ij}^{-1} \langle \xi_j B \rangle \\ \int_0^\infty \langle B \xi_i(t) \rangle e^{-pt} dt &= \sum_j (M + pI)_{ij}^{-1} \langle B \xi_j \rangle, \end{aligned} \quad (25)$$

where I is the identity matrix. By setting $B = \xi_k$ and $p = \pm i\omega$ in equation (25), we derive the basic formula

$$\tilde{R}_{ik} = \int_0^\infty \langle [\xi_i(t), \xi_k] \rangle e^{-i\omega t} dt = \sum_j (M + i\omega I)_{ij}^{-1} \langle [\xi_j, \xi_k] \rangle, \quad (26)$$

allowing us to calculate from the linearized drift matrix \tilde{R} , of which the response functions R of equation (17), is a submatrix.

By introducing the matrix C^0 of equal time commutators

$$C_{ij}^0 = \langle [\xi_i, \xi_j] \rangle, \quad (27)$$

equation (26) can be written in a matrix form

$$\tilde{R} = (M + i\omega I)^{-1} C^0. \quad (28)$$

In order to calculate the correlation matrix (18), we split the integration interval into two parts and transform it to have positive times in each part

$$S_{ij} = \int_0^\infty \langle :: \beta_i \beta_j(t) :: \rangle e^{i\omega t} dt + \int_0^\infty \langle :: \beta_i(t) \beta_j :: \rangle e^{-i\omega t} dt, \quad (29)$$

where we assumed that there is translational invariance in time. The matrix S_{ij} defined by equation (18) is a submatrix of a matrix \tilde{S}_{ij} which refers to the whole set of the system operators

$$\tilde{S}_{ij} = \int_0^\infty \langle :: \xi_i \xi_j(t) :: \rangle e^{i\omega t} dt + \int_0^\infty \langle :: \xi_i(t) \xi_j :: \rangle e^{-i\omega t} dt, \quad (30)$$

where the normal ordering for the atomic operators can be appropriately defined, but is irrelevant for the results which concern the field spectra. Each term of equation (30) can be evaluated by using the regression theorem like before. By introducing the matrix C^N of equal-times normally ordered correlations

$$C_{ij}^N = \langle : \xi_i \xi_j : \rangle, \quad (31)$$

we can express the result in the form

$$\begin{aligned} \tilde{S} &= (M + i\omega I)^{-1} C^N + C^N (M^T - i\omega I)^{-1} \\ &= (M + i\omega I)^{-1} D (M^T - i\omega I)^{-1}, \end{aligned} \quad (32)$$

where we introduced the diffusion matrix D

$$D = C^N (M^T - i\omega I) + (M + i\omega I) C^N = C^N M^T + M C^N, \quad (33)$$

which corresponds to the diffusion matrix in the Fokker-Planck equation in the Glauber-P representation [44]. We note that the calculation of C_{ij}^0 is straightforward, because the commutator $[\xi_i, \xi_j]$ is typically either a c -number or a linear combination of operators ξ_i themselves. On the other hand, the quantities C_{ij}^N are not easily accessible because they are expectation values of products of fluctuation operators. In the following section we show how one can obtain the diffusion matrix D , so that the matrix \tilde{S} can be calculated.

5.2 Calculation of the diffusion matrix

In the Schödinger picture, the dynamics is described by the ME (2). If one adopts, instead, the Heisenberg picture, the time evolution is governed by a set of quantum Langevin equations [44]

$$\frac{d\xi_i}{dt} = A_i + \Gamma_i(t), \quad (34)$$

where A_i are the drift terms, and Γ_i are the stochastic force terms, such that

$$\langle \Gamma_i(t) \rangle = 0, \quad \langle \Gamma_i(t) \Gamma_j(t') \rangle = 2G_{ij} \delta(t - t'). \quad (35)$$

The coefficients G_{ij} can be obtained by using the generalized Einstein formula [44]

$$G_{ij} = \frac{d}{dt} \langle \xi_i \xi_j \rangle - \langle A_i \xi_j \rangle - \langle \xi_i A_j \rangle. \quad (36)$$

In the linearized approximation around the stationary state, the drift terms read

$$A_i = - \sum_j M_{ij} \xi_j. \quad (37)$$

At the steady state one obtains from equations (36, 37)

$$G_{jk} = \sum_n M_{jn} \langle \xi_n \xi_k \rangle + \sum_n M_{kn} \langle \xi_j \xi_n \rangle. \quad (38)$$

Let us assume that in general the fluctuation operators ξ_i are ordered in such a way that the sequence ξ_1, ξ_2, \dots is in normal order. For example, if the dynamics involves only the fields 1 and 2, we assume that $\{\xi_i\} = a_1^\dagger, a_1, a_2^\dagger, a_2, \dots$. If we start from equation (38) and set the operators in normal order in the correlation, we obtain

$$G_{jk} - \sum_{n>k} M_{jn} \langle [\xi_n, \xi_k] \rangle - \sum_{n<j} M_{kn} \langle [\xi_j, \xi_n] \rangle = \sum_n M_{jn} C_{nk}^N + \sum_n M_{kn} C_{jn}^N, \quad (39)$$

where C_{ij}^N is defined by equation (31). By introducing the triangular matrix C_*

$$\begin{aligned} (C_*)_{ij} &= C_{ij}^0 & j < i \\ (C_*)_{ij} &= 0 & j \geq i \end{aligned} \quad (40)$$

one has:

$$G - MC_* - C_* M^T = MC^N + C^N M^T = D. \quad (41)$$

Then the drift matrix M , the equal times commutator matrix C^0 and the matrix G can be used to compute the steady state linearized diffusion matrix D .

When the ME is of the Linblad form (2) the term A has the form (3) and one obtains that

$$G_{ij} = \sum_l \kappa_l \langle [c_l^\dagger, \xi_i] [\xi_j, c_l] \rangle \quad (42)$$

where again the sum is over all the system operators c_j coupled to the reservoir. In models that includes only field variables, $c_l = a_l$ ($l = 1, 2$).

6 Dispersive model

As an example, we apply our formulation to a simple model, which describes a nonlinear Kerr type coupling of two field modes in the dispersive limit. This model as QND scheme has been discussed in some special cases [14–20, 29, 43]. Here we study its squeezing and correlation spectra in more general cases. The master equation of the system in the interaction picture is

$$\frac{d\rho}{dt} = \frac{1}{i\hbar} [H, \rho] + \sum_{j=1,2} \kappa_j ([a_j, \rho a_j^\dagger] + [a_j \rho, a_j^\dagger]) \quad (43)$$

with

$$H = \hbar \sum_{j=1}^2 \kappa_j \Delta_j a_j^\dagger a_j + \hbar g a_1^\dagger a_1 a_2^\dagger a_2 + i\hbar \sum_{j=1}^2 (\epsilon_j a_j^\dagger - \epsilon_j^* a_j), \quad (44)$$

where $\Delta_j = (\omega_{c_j} - \omega_j)/\kappa_j$ is the normalized empty cavity detuning (ω_{c_j} is the cavity frequency and ω_j is the frequency of the input field), $\kappa_j = cT_j/(2\mathcal{L})$ is the cavity decay rate for the j th mode T_j being the transmission of the cavity mirror and \mathcal{L} being the cavity length; ϵ_j is the amplitude for the j th coherent driving field, and g is the nonlinear coupling constant. We define normalized variables as follows:

$$\begin{aligned} A_1 &= \sqrt{g/\kappa_2} \langle a_1 \rangle, & A_2 &= \sqrt{g/\kappa_1} \langle a_2 \rangle, \\ E_1 &= \sqrt{g/\kappa_2} (\epsilon_1/\kappa_1), & E_2 &= \sqrt{g/\kappa_1} (\epsilon_2/\kappa_2), \\ \tau &= \kappa_2 t, & \eta &= g/\kappa_2, & \kappa &= \kappa_1/\kappa_2. \end{aligned} \quad (45)$$

The classical stationary solution of the system, obtained by neglecting quantum fluctuations, is

$$\begin{aligned} A_1 &= E_1 / [1 + i(\Delta_1 + |A_2|^2)] = E_1 \cos \phi_1 e^{-i\phi_1} \\ A_2 &= E_2 / [1 + i(\Delta_2 + |A_1|^2)] = E_2 \cos \phi_2 e^{-i\phi_2}, \end{aligned} \quad (46)$$

where ϕ_j is the nonlinear phase shift of the intracavity mode A_j with respect to the input field E_j . Each ϕ_j consists of two parts: the empty cavity detuning and the nonlinear frequency shift $|A_{3-j}|^2$, *i.e.*

$$\begin{aligned} \phi_1 &= \tan^{-1}(\Delta_1 + |A_2|^2), \\ \phi_2 &= \tan^{-1}(\Delta_2 + |A_1|^2). \end{aligned} \quad (47)$$

Note that $-\pi/2 < \phi_{1,2} < \pi/2$. In the case $\phi_j = 0$ one has the nonlinear cavity resonance for the mode j , in order to satisfy this condition, a negative detuning (that is laser field frequency larger than that of the corresponding cavity mode) must be taken. For this pure dispersive model, the factor $\cos \phi_{1,2}$ accounts exactly for the ratio between the incident and internal field amplitudes (see Eq. (46)). Due to this circumstance, it is very convenient to use $\cos \phi_1$ and $\cos \phi_2$ as the system variables. We set E_1 real and positive, while E_2 may have a phase δ , *i.e.* $E_2 = |E_2| e^{i\delta}$. The phases for the intracavity modes A_1 and A_2 are then $-\phi_1$ and $-\phi_2 + \delta$, respectively.

$$M = \begin{pmatrix} \kappa e^{i\phi_1} / \cos \phi_1 & 0 & i\kappa r_c e^{-i(\phi_1 - \phi_2 + \delta)} & i\kappa r_c e^{-i(\phi_1 + \phi_2 - \delta)} \\ 0 & \kappa e^{-i\phi_1} / \cos \phi_1 & -i\kappa r_c e^{i(\phi_1 + \phi_2 - \delta)} & -i\kappa r_c e^{i(\phi_1 - \phi_2 + \delta)} \\ i r_c e^{i(\phi_1 - \phi_2 + \delta)} & i r_c e^{-i(\phi_1 + \phi_2 - \delta)} & e^{i\phi_2} / \cos \phi_2 & 0 \\ -i r_c e^{i(\phi_1 + \phi_2 - \delta)} & -i r_c e^{-i(\phi_1 - \phi_2 + \delta)} & 0 & e^{-i\phi_2} / \cos \phi_2 \end{pmatrix}, \quad (48)$$

$$D = \eta r_c \begin{pmatrix} 0 & 0 & -ie^{-i(\phi_1 + \phi_2 - \delta)} & 0 \\ 0 & 0 & 0 & ie^{i(\phi_1 + \phi_2 - \delta)} \\ -ie^{-i(\phi_1 + \phi_2 - \delta)} & 0 & 0 & 0 \\ 0 & ie^{i(\phi_1 + \phi_2 - \delta)} & 0 & 0 \end{pmatrix}, \quad (49)$$

For a single-ended cavity the phases of the two output fields are correspondingly $-2\phi_1$ and $-2\phi_2 + \delta$ [43]. As a matter of fact, we will see that δ plays no role in the results.

Now we linearize the system around the stationary solution and obtain the drift matrix M and the diffusion matrix D which read:

see equations (48, 49) above

where r_c is defined as the cross-intracavity intensity and r is the cross-input intensity:

$$r_c \equiv |A_1 A_2| = r \cos \phi_1 \cos \phi_2, \quad r = |E_1 E_2|. \quad (50)$$

7 Steady state and stability

The steady state solution for the intracavity fields as a function of input fields amplitudes and cavity detunings are given by (46). Experimentally, different steady state configurations can be explored by varying length of the cavity which implies a variation in the empty cavity detuning:

$$\Delta_1 = \Delta_{01} + \delta\Delta_1 \quad (51)$$

$$\Delta_2 = \Delta_{02} + \delta\Delta_2, \quad (52)$$

where Δ_{01} and Δ_{02} are the initial cavity detunings corresponding to a given cavity length and $\delta\Delta_1$ and $\delta\Delta_2$ are the variation of the cavity detunings due to a variation of the cavity length. As can be easily seen shown from the definition of the empty cavity detunings Δ_i after equation (44), the $\delta\Delta_j$ satisfy

$$\delta\Delta_1 = A\delta\Delta_2 \quad \text{with} \quad A = \frac{\lambda_2 T_2}{\lambda_1 T_1}. \quad (53)$$

From equations (47, 46) one has:

$$\delta\Delta_1 = \tan \phi_1 - (\Delta_{01} + |E_2|^2 \cos^2 \phi_2) \quad (54)$$

$$\delta\Delta_2 = \tan \phi_2 - (\Delta_{02} + |E_1|^2 \cos^2 \phi_1). \quad (55)$$

One can explore numerically the steady state solutions obtained by varying ϕ_1 and ϕ_2 in $[-\pi/2, \pi/2]$ subject to the condition (53), which corresponds experimentally

to varying the cavity length. An example is shown in Figure 1a where the normalized intracavity field intensities $|A_j|^2/E_j^2 = \cos^2 \phi_j$ are represented as a function of the cavity length or $\delta\Delta_1$ for $\Delta_{01} = -16$, $\Delta_{02} = 0$, $E_1 = 0.2$, $E_2 = 4$, $A = 1$. We notice that the intense field (field 2) is basically not perturbed by the presence of the weak field (field 1) and shows its resonance in $\delta\Delta_2 = -\Delta_{02} = 0$. The weak field on the other hand exhibits two resonances: one approximately unperturbed resonance at $\delta\Delta_1 = -\Delta_{01} = 16$ and a second resonance in correspondence to the resonance of the strong field at $\delta\Delta_1 = 0$. We will see that the simultaneous resonance condition for the two fields is favorable for QND. As we learn from this simple Kerr model, in this asymmetric situation for the fields intensities, the two fields can be brought simultaneously at resonance by choosing a distance between the empty cavity resonances ($\Delta_{01} - \Delta_{02}$) equal to the non linear phase shift of the weak field. A similar configuration has actually been realized experimentally see [29,37]. If we now increase the input field intensity the steady state solution can become bistable as shown in Figure 1b. In this case not all the steady state solutions are accessible. The stability condition which can be found by a linear stability analysis is:

$$d_\phi = \frac{1}{\cos^2 \phi_1 \cos^2 \phi_2} - r^2 \sin 2\phi_1 \sin 2\phi_2 > 0. \quad (56)$$

The condition $d_\phi = 0$ corresponds to the turning point of bistable steady-state curve in Figure 1b. Bistability arises only for $r > 1.53961$. The stable and unstable domains in the plane $(\cos \phi_1, \cos \phi_2)$ are shown in Figure 2 for several values of r . The curves correspond to the condition $d_\phi(0) = 0$ and there is stability (instability) in the region outside (inside) the curves. For large r , the boundary of the unstable region gets very close, although not exactly coincident, to the nonlinear cavity resonances $\phi_{1,2} = 0$. Note that in Figure 2 we have assumed that ϕ_1 and ϕ_2 have the same sign.

8 QND and squeezing at zero frequency

We now apply the formulas for quantum correlations of the previous section of the paper to study the squeezing

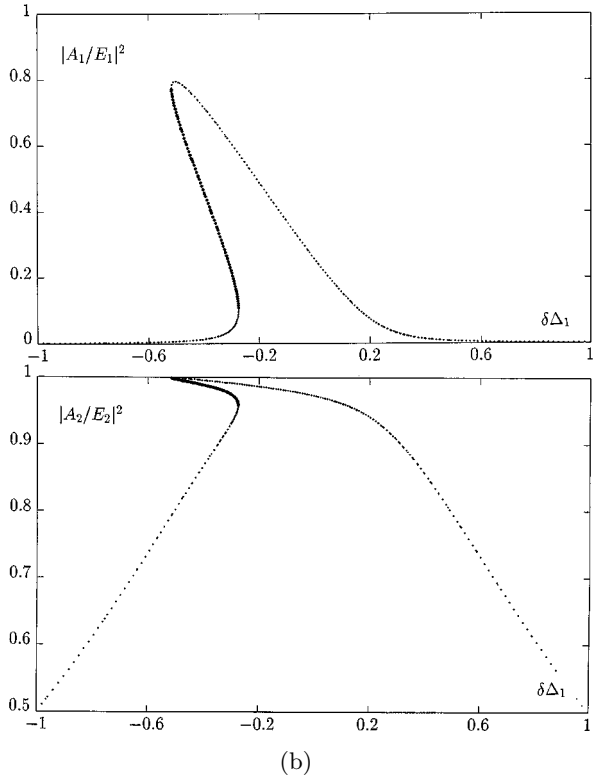
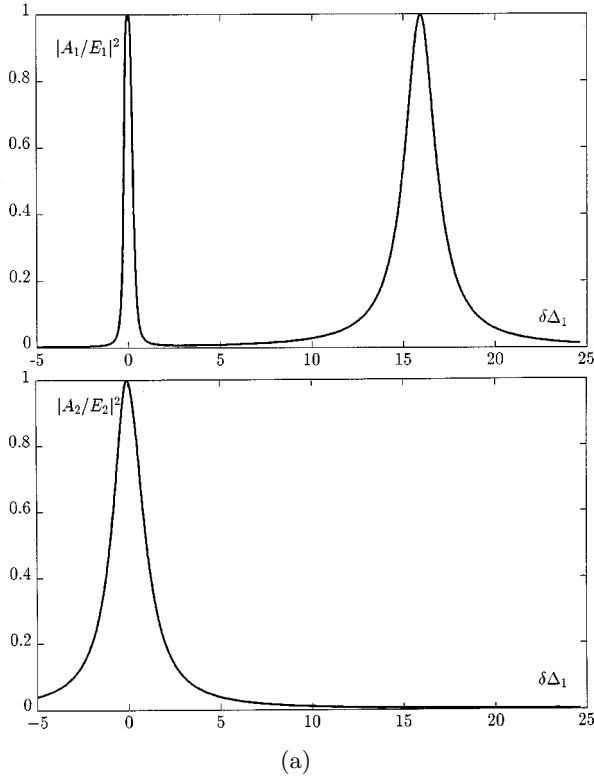


Fig. 1. Normalized steady state intracavity intensities $|A_i|^2/|E_i|^2$ ($i = 1, 2$) as a function of the cavity detuning $\delta\Delta_1$ (cavity length) for (a) $\Delta_{01} = -16$, $\Delta_{02} = 0$, $E_1 = 0.2$, $E_2 = 4$ $A = 1$ and (b) $\Delta_{01} = -64$, $\Delta_{02} = 0$, $E_1 = 0.8$, $E_2 = 8$ $A = 1$. The darker dots in (b) indicate unstable solutions.

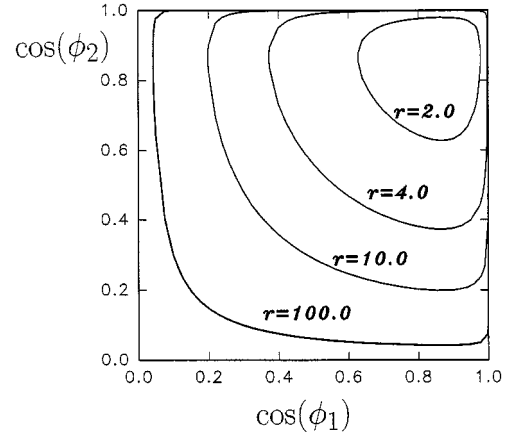


Fig. 2. Loci of the bistability transition points in the plane $(\cos \phi_1, \cos \phi_2)$ for $r = 2, 4, 10$, and 100 . ϕ_1 and ϕ_2 have the same sign.

and QND properties of the simple Kerr model. In this subsection we consider the correlations at zero frequency for general parameters to obtain simple formulas and optimize the squeezing and QND effects. In the next one we focus on the case of nonlinear double-resonance $\phi_1 = \phi_2 = 0$, which turns out to be the best condition for QND, and we study the frequency spectra.

8.1 Choice of the quadrature phases

By using equations (21, 32, 48, 49) and taking into account the scale factors in equation (45), we obtain the squeezing spectra for the output fields and the QND correlations at zero frequency for general parameters and intracavity fields amplitudes. We have put the analytic expression for those quantities in the appendix.

The noise spectra for the fields, as well as the QND correlations depend on the angles $\phi_{1,2}$, related to the cavity resonance conditions for the two fields, and on the value of $\Delta\theta_j^{\text{out}}$ ($j = 1, 2$) which describe the difference between the phase of the quadrature x_j^{out} (see Eq. (7)) and the phase of the j th stationary output field

$$\begin{aligned}\Delta\theta_1^{\text{out}} &= \theta_1^{\text{out}} + 2\phi_1 \\ \Delta\theta_2^{\text{out}} &= \theta_2^{\text{out}} + 2\phi_2 - \delta,\end{aligned}\quad (57)$$

and similarly,

$$\begin{aligned}\Delta\theta_1^{\text{in}} &= \theta_1^{\text{in}} \\ \Delta\theta_2^{\text{in}} &= \theta_2^{\text{in}} - \delta.\end{aligned}\quad (58)$$

Note that the quantity d_ϕ defined in (56) appears in the formula for noise spectra and QND correlations. From the expression of $\langle x_1^{\text{out}} x_2^{\text{in}} \rangle$ in the Appendix it is clear that the correlation between the outgoing meter and the incoming signal reaches its maximum when

$$\Delta\theta_1^{\text{out}} = \pi/2, \quad \Delta\theta_2^{\text{in}} = 0. \quad (59)$$

If, in addition, we set

$$\Delta\theta_2^{\text{out}} = 0, \quad (60)$$

the amplitude fluctuations of the signal remain always at shot noise level¹, (see Eq. (A.1) in the Appendix), so that

$$V_c(x_2^{\text{out}}|x_1^{\text{out}}) = \frac{1}{4}(1 - C_3^2). \quad (61)$$

Furthermore, with the same choice of the quadrature phases one has

$$C_1^2(0) = \frac{16r^2}{d_\phi^2(0) + 16r^2(1 + r^2 \cos^4\phi_1 \sin^2 2\phi_2)}, \quad (62)$$

and

$$\langle x_2^{\text{out}} x_2^{\text{in}} \rangle_{\text{sym}} = -1/4, \quad (63)$$

$$\langle x_2^{\text{out}} x_1^{\text{out}} \rangle_{\text{sym}} = -r/d_\phi(0), \quad (64)$$

which implies that

$$C_2^2(0) = 1, \quad C_3^2(0) = C_1^2(0) \quad (65)$$

which show that the first and the third criteria *effectiveness of the measurement and QSP* can be satisfied simultaneously, while the second criterion *non demolition of the signal* is always satisfied.

As far as the squeezing is concerned, it is convenient to define an optimized squeezing obtained by selecting an optimum quadrature phase. Such “optimized” squeezing is given by

$$V_{\text{opt}}(x_2^{\text{out}}, 0) = \frac{1}{4} + \frac{1}{2}\kappa_2\{S_{34}(0) + S_{43}(0) - 2|S_{33}(0)|\}, \quad (66)$$

and the corresponding quadrature phase is

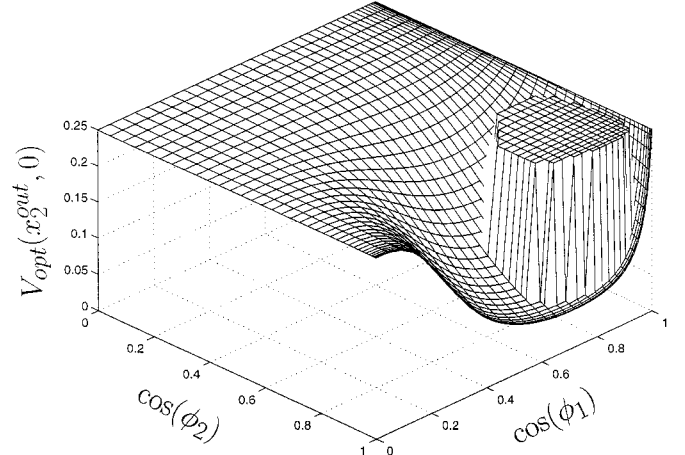
$$\exp[-2i\theta_{2,\text{opt}}^{\text{out}}] = S_{33}^*(0)/|S_{33}(0)| \quad (67)$$

we give the explicit formula for $V_{\text{opt}}(x_2^{\text{out}}, 0)$ and $\theta_{2,\text{opt}}^{\text{out}}$ in the Appendix.

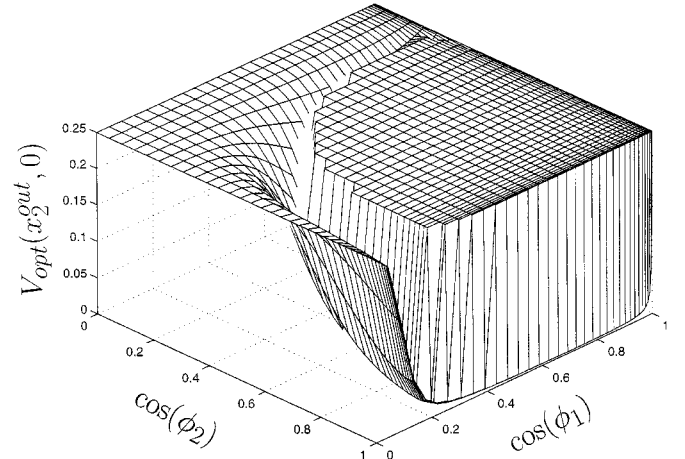
8.2 Optimization of Squeezing and QND effects

The dependence of the noise spectrum $V_{\text{opt}}(x_2^{\text{out}}, 0)$ on the resonance parameters $\phi_{1,2}$, for two different values of the cross-input intensity r , is shown in Figures 3a and 3b, while the coefficient C_1^2 as a function of the same variables is shown in Figures 4a and 4b. In these figures, as in Figure 2, ϕ_1 and ϕ_2 have the same sign. We are interested only in the stable region where $d_\phi > 0$, for this reason in the *unstable* region we have put arbitrarily $V_{\text{opt}}(x_2^{\text{out}}, 0) = 1/4$ and $C_1^2 = 0$. The most interesting points are in the stable region close to the border of the unstable domain. In particular the best squeezing appears at $\phi_2 = 0$ at which the stationary solution is always stable.

¹ This conclusion, obtained for $\omega = 0$, does not hold for non zero frequencies where amplitude quadrature squeezing can be obtained [29].



(a)



(b)

Fig. 3. Optimum squeezing at zero frequency for mode 2 as function of $\cos\phi_1$ and $\cos\phi_2$ for (a) $r = 2$ and (b) $r = 10$. ϕ_1 and ϕ_2 have the same sign.

8.2.1 Close to the instability border

We can use our formula (62), and (A.5, A.6) in the Appendix to get simple quantitative estimates of the squeezing and QND correlations close to instability boundary. By setting $d_\phi \rightarrow 0$ in those formulas we obtain:

$$V_{\text{opt}}(x_2^{\text{out}}, 0) \rightarrow \frac{1}{4(1 + \cot\phi_2 \tan\phi_1)} \quad (68)$$

$$\Delta\theta_{2,\text{opt}}^{\text{out}} \rightarrow 0 \quad (68)$$

$$C_1^2(0) \rightarrow \frac{1}{1 + \cot\phi_1 \tan\phi_2}. \quad (69)$$

Equation (68) shows that close to the instability boundary, the perfect squeezing limit for mode 2 occurs either at $\phi_2 \rightarrow 0$ or $\phi_1 \rightarrow \pm\pi/2$, and approximately in the amplitude quadrature. (Note that the limit $d_\phi(0) \rightarrow 0$ ensures $\cot\phi_2 \tan\phi_1 > 0$.) According to Figure 2, the instability

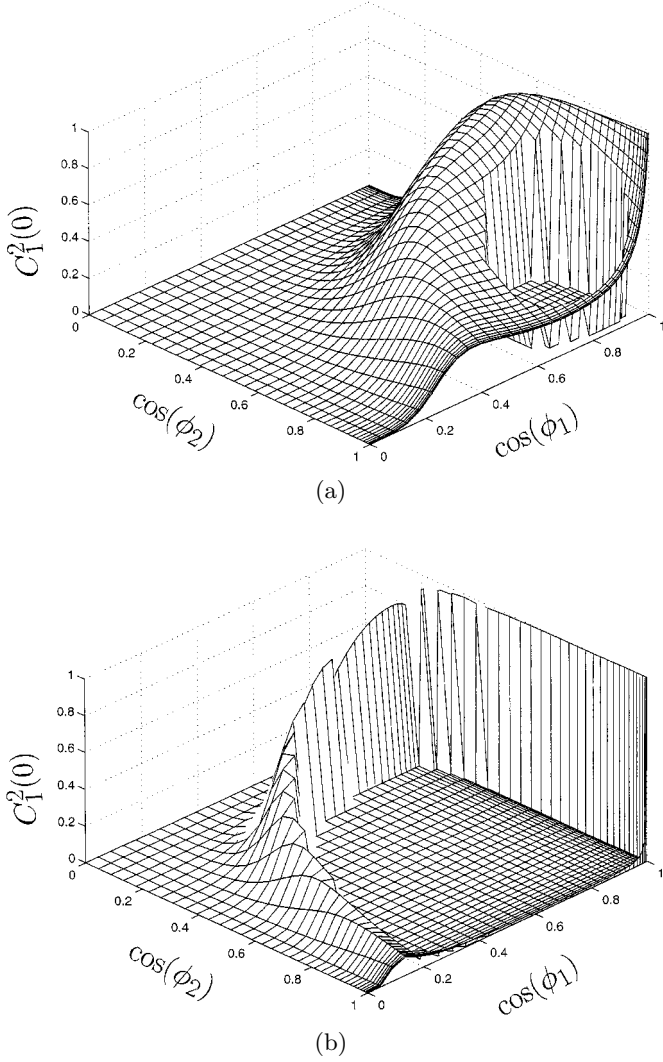


Fig. 4. $C_{1,3}^2(0)$ as function of $\cos \phi_1$ and $\cos \phi_2$ for given incident parameters: (a) $r = 2$ and (b) $r = 10$. ϕ_1 and ϕ_2 have the same sign.

boundary gets close to $\phi_2 = 0$ provided that r is not too small. On the other hand the other condition $\phi_1 \rightarrow \pm\pi/2$ would require much higher input intensities (see Eq. (46)) and seems thus difficult to realize.

Equation (69) shows that the same conditions, $\phi_2 \rightarrow 0$ or $\phi_1 \rightarrow \pm\pi/2$, provide good QND coupling.

8.2.2 Resonance for the signal

Since the limit $\phi_2 \rightarrow 0$ seems most favorable, we substitute directly $\phi_2 = 0$ in (62, A.5, A.6) to obtain:

$$C_1^2(0) = \frac{16r^2}{\cos^{-4}\phi_1 + 16r^2} \quad (70)$$

and a still rather complicated expression for $V_{\text{opt}}(x_2^{\text{out}}, 0)$ and $\Delta\theta_{2,\text{opt}}^{\text{out}}$. However, if $1 + r^2 \sin^2 2\phi_1 \gg |\tan \phi_1|$ meaning a large value of r and a suitable ϕ_1 well detuned from 0

and $\pm\pi/2$, the expression for $V_{\text{opt}}(x_2^{\text{out}}, 0)$ is simplified as

$$V_{\text{opt}}(x_2^{\text{out}}, 0) \approx \frac{1}{4(1 + r^2 \sin^2 2\phi_1)}$$

$$\Delta\theta_{2,\text{opt}}^{\text{out}} \approx 0. \quad (71)$$

In such conditions a large amount of squeezing is found in a quadrature close to the amplitude quadrature and, as we see from equation (70) a good QND coupling is found at the same time.

We can ask ourselves what happens then to the noise properties of the other field. If one sets $\phi_2 = 0$ in equation (A.1) in the Appendix, one gets:

$$V(x_1^{\text{out}}, 0) = \frac{1}{4} + 4r^2 \sin^2 \Delta\theta_1^{\text{out}} \cos^4 \phi_1. \quad (72)$$

The output fluctuations for the meter field are always above (or equal to) the shot noise level, reaching the minimum in the amplitude quadrature and the maximum in the phase quadrature. This is easy to understand from the fact that the two fields are strongly coupled in a QND sense. The noise on the meter can in fact be interpreted as measurement back-action noise and the squeezing in the signal field as back-action induced squeezing [29].

8.2.3 Resonance for the signal and the meter

As far as the QND is concerned the best coupling is however obtained at the nonlinear double resonance: $\phi_1 = \phi_2 = 0$, in which case

$$C_1^2(0) = \frac{16r^2}{1 + 16r^2}. \quad (73)$$

9 QND and squeezing spectra at double resonance

When the double resonance condition $\phi_1 = \phi_2 = 0$ condition is satisfied, the noise spectrum for both modes is

$$V(x_j^{\text{out}}, \bar{\omega}) = \frac{1}{4} + \frac{4\kappa^2 r^2 \sin^2 \Delta\theta_j^{\text{out}}}{[\bar{\omega}^4 + \bar{\omega}^2(\kappa^2 + 1) + \kappa^2]} \quad (j = 1, 2), \quad (74)$$

where $\bar{\omega} = \omega/\kappa_2$. The minimum noise is the shot noise level obtained for the amplitude quadrature, so that the double nonlinear resonance condition is not favorable to squeezing.

The correlation spectra are very simple:

$$C_1^2(\bar{\omega}) = C_3^2(\bar{\omega}) = \frac{16\kappa^2 r^2}{16\kappa^2 r^2 + [\bar{\omega}^4 + \bar{\omega}^2(\kappa^2 + 1) + \kappa^2]}$$

$$= 1 - \frac{1}{4V(x_1^{\text{out}}, \bar{\omega}) \Delta\theta_1^{\text{out}} = \pi/2},$$

$$C_2^2(\bar{\omega}) = 1, \quad (75)$$

where we used equations (59, 60), and $V(x_1^{\text{out}}, \bar{\omega})_{\Delta\theta_1^{\text{out}}=\pi/2}$ is defined by equation (74) with $\Delta\theta_1^{\text{out}} = \pi/2$. The conditional variance is

$$V_c(x_2^{\text{out}}|x_1^{\text{out}}) = \frac{1}{4}[1 - C_3^2(\bar{\omega})] = \frac{1}{16V(x_1^{\text{out}}, \bar{\omega})_{\Delta\theta_1^{\text{out}}=\pi/2}}. \quad (76)$$

We get then similar results as in the zero frequency case: the first and the third criteria can be satisfied at the same time and the second is fully satisfied for all frequencies.

Equations (75, 76) give a direct relation between the noise spectrum of the meter beam and the QND criteria — the more excess noise in the phase quadrature for the meter field, the better QND performance. This excess noise in the phase of the meter field is in fact the back action noise introduced in the system by the measurement according to quantum mechanical laws.

10 Conclusion

We have presented in detail a method based on the quantum regression theorem to derive input-output correlation spectra in a linearized system. We have shown that the QND coefficients can be expressed in terms of response and correlation function which can be simply calculated starting from the drift matrix and the matrix of equal time commutators of the system variables.

By using this method, we have discussed an ideal dispersive model, and analyzed the squeezing spectra and QND performance of the simple dispersive model. Simple relations among the squeezing spectra, the QND correlations and the instability have been revealed in our analytical results.

One of us, Wang Kaige, acknowledges financial support from the National Natural Science Foundation of China, No. 19774013, and the ICTP Program of T&R, Trieste, Italy. A.S. thanks Yvan Castin for very useful comments on the manuscript.

Appendix

In this appendix we give the analytical expressions for the squeezing and the QND correlations at zero frequency for the dispersive model for general parameters.

- Squeezing of the output fields

$$V(x_1^{\text{out}}, 0) = \frac{1}{4} + 4r^2 \sin \Delta\theta_1^{\text{out}} [\sin(\phi_2 + \Delta\theta_1^{\text{out}}) / \cos \phi_2 - 4r^2 \cos^3 \phi_1 \sin(\phi_1 - \Delta\theta_1^{\text{out}}) \cos^2 \phi_2 \sin^2 \phi_2] / d_\phi^2, \quad (A.1)$$

(and a similar expression holds for $V(x_2^{\text{out}}, 0)$ with the indices 1 and 2 exchanged).

- Correlation between the input signal and the meter output

$$|\langle x_1^{\text{out}} x_2^{\text{in}} \rangle_{\text{sym}}^{\omega=0}|^2 = r^2 \sin^2 \Delta\theta_1^{\text{out}} \cos^2 \Delta\theta_2^{\text{in}} / d_\phi^2. \quad (A.2)$$

- Correlation between the input and output signal

$$\begin{aligned} \langle x_2^{\text{out}} x_2^{\text{in}} \rangle_{\text{sym}} &= \frac{1}{4} \cos(\Delta\theta_2^{\text{in}} - \Delta\theta_2^{\text{out}} + 2\phi_2) \\ &\quad - \frac{1}{d_\phi} \left[\frac{\cos(\Delta\theta_2^{\text{in}} - \Delta\theta_2^{\text{out}} + \phi_2)}{2 \cos^2 \phi_1 \cos \phi_2} \right. \\ &\quad \left. + r^2 \sin 2\phi_1 \cos^2 \phi_2 \cos(\Delta\theta_2^{\text{in}} + \phi_2) \sin(\Delta\theta_2^{\text{out}} - \phi_2) \right]. \end{aligned} \quad (A.3)$$

- Correlation between the output meter and output signal

$$\begin{aligned} \langle x_2^{\text{out}} x_1^{\text{out}} \rangle_{\text{sym}} &= \\ &\quad \frac{r}{d_\phi^2} \{ r^2 \cos \phi_1 \cos \phi_2 [\sin(\Delta\theta_1^{\text{out}} + \Delta\theta_2^{\text{out}} + \phi_1 + \phi_2) \\ &\quad - 3 \sin(\Delta\theta_1^{\text{out}} + \Delta\theta_2^{\text{out}} - \phi_1 - \phi_2) \\ &\quad + 2 \sin(\Delta\theta_1^{\text{out}} + \Delta\theta_2^{\text{out}}) \cos(\phi_1 - \phi_2) \\ &\quad - 4 \cos(\Delta\theta_1^{\text{out}} - \Delta\theta_2^{\text{out}}) \sin(\phi_1 + \phi_2)] - \frac{\sin(\Delta\theta_1^{\text{out}} + \Delta\theta_2^{\text{out}})}{\cos^2 \phi_1 \cos^2 \phi_2} \}. \end{aligned} \quad (A.4)$$

- Optimized quadrature squeezing

$$\begin{aligned} V_{\text{opt}}(x_2^{\text{out}}, 0) &= \frac{1}{4} + 2r^2 \{ (1 + r^2 \cos^4 \phi_2 \sin^2 2\phi_1) \\ &\quad - [(1 + r^2 \cos^4 \phi_2 \sin^2 2\phi_1)^2 \\ &\quad + \frac{1}{4} \cos^4 \phi_2 \sin^2 2\phi_1 d_\phi^2(0)]^{1/2} \} / d_\phi^2(0), \end{aligned} \quad (A.5)$$

$$\begin{aligned} \Delta\theta_{2,\text{opt}}^{\text{out}} &= \\ &\quad - \frac{1}{2} \arctan \left[\frac{1}{2} \cos^2 \phi_2 \sin 2\phi_1 d_\phi(0) / (1 + r^2 \cos^4 \phi_2 \sin^2 2\phi_1) \right]. \end{aligned} \quad (A.6)$$

References

1. M.C. Teich, B.A. Saleh, *Quant. Opt.* **1**, 153 (1989).
2. R. Loudon, P.L. Knight, *J. Mod. Opt.* **34**, 709 (1987).
3. H. Yuen, *Phys. Rev. A* **13**, 2226 (1976).
4. H. Yuen, J.H. Shapiro, *Opt. Lett.* **4**, 334 (1979).
5. G.J. Milburn, D.F. Walls, *Opt. Commun.* **39**, 401 (1981).
6. B. Yurke, *Phys. Rev. A* **29**, 408 (1984).
7. M.J. Collett, D.F. Walls, *Phys. Rev. A* **32**, 2887 (1985).
8. L.M. Narducci, W.W. Eidson, P. Furcinitti, D.C. Eteson, *Phys. Rev. A* **16**, 1665 (1980).
9. R. Bonifacio, L.A. Lugiato, *Phys. Rev. A* **18**, 1129 (1978).
10. P. Drummond, D.F. Walls, *J. Phys. A* **13**, 725 (1980).

11. P. Galatola, L.A. Lugiato, M. Vadicchino, N.B. Abraham, *Opt. Commun.* **69**, 414 (1989).
12. P. Galatola, L.A. Lugiato, M. Vadicchino, N.B. Abraham, *Opt. Commun.* **69**, 419 (1989).
13. L.A. Lugiato, P. Galatola, L.M. Narducci, *Opt. Commun.* **76**, 276 (1990).
14. G.J. Milburn, D.F. Walls, *Phys. Rev. A* **28**, 2065 (1983).
15. N. Imoto, H.A. Haus, Y. Yamamoto, *Phys. Rev. A* **32**, 2287 (1985).
16. R.M. Shelby, M.D. Levenson, *Opt. Commun.* **64**, 553 (1987).
17. P. Alsing, G.J. Milburn, D.F. Walls, *Phys. Rev. A* **37**, 2970 (1988).
18. P. Grangier, J.-F. Roch, *Quant. Opt.* **1**, 17 (1989).
19. P. Grangier, J.-F. Roch, S. Reynaud, *Opt. Commun.* **72**, 387 (1989).
20. C.A. Blockley, D.F. Walls, *Opt. Commun.* **79**, 241 (1990).
21. M.J. Holland, M.J. Collett, D.F. Walls, *Phys. Rev. A* **42**, 2995 (1990).
22. P. Grangier, J.-F. Roch, G. Roger, *Phys. Rev. Lett.* **66**, 1418 (1991).
23. P. Grangier, J.-M. Courty, S. Reynaud, *Opt. Commun.* **89**, 99 (1992).
24. J.-F. Roch, G. Roger, P. Grangier, J.-M. Courty, S. Reynaud, *Appl. Phys. B* **55**, 291 (1992).
25. P. Grangier, *Phys. Rep.* **219**, 121 (1992).
26. J.-Ph. Poizat, M.J. Collett, D.F. Walls, *Phys. Rev. A* **45**, 5171 (1992).
27. K.M. Gheri, P. Grangier, J.-Ph. Poizat, D.F. Walls, *Phys. Rev. A* **46**, 4276 (1992).
28. M. Dance, M.J. Collett, D.F. Walls, *Phys. Rev. A* **48**, 1532 (1993).
29. P. Grangier, J.-Ph. Poizat, P. Grelu, F. Castelli, L.A. Lugiato, A. Sinatra, *J. Mod. Opt.* **41**, 2241 (1994).
30. J.-Ph. Poizat, J.-F. Roch, P. Grangier, *Ann. Phys. Fr.* **19**, 265 (1994).
31. P. Grangier, J.-Ph. Poizat, J.-F. Roch, *Phys. Scripta T* **51**, 51 (1994).
32. K. Bencheikh, A. Levenson, Ph. Grangier, O. Lopez, *Phys. Rev. Lett.* **75**, 3422 (1995).
33. Yang Guojian, Wang Kaige, *Opt. Commun.* **137**, 151 (1997).
34. Yang Guojian, Wang Kaige, *J. Opt. Soc. Am. B* **14**, 1550 (1997).
35. R. Bruckmeier, K. Schneider, S. Schiller, J. Mlynek, *Phys. Rev. Lett.* **78**, 1243 (1997).
36. R. Bruckmeier, H. Hansen, S. Schiller, *Phys. Rev. Lett.* **79**, 1463 (1997).
37. A. Sinatra, J.-F. Roch, K. Vigneron, Ph. Grelu, J.-Ph. Poizat, Kaige Wang, P. Grangier, *Phys. Rev. A* **57**, 2980 (1998).
38. S. Reynaud, C. Fabre, E. Giacobino, A. Heidmann, *Phys. Rev. A* **40**, 1440 (1989).
39. L. Hilico, C. Fabre, S. Reynaud, E. Giacobino, *Phys. Rev. A* **46**, 4397 (1992).
40. S. Reynaud, A. Heidmann, *Opt. Commun.* **71**, 209 (1991).
41. J.M. Courty, P. Grangier, L. Hilico, S. Reynaud, *Opt. Commun.* **83**, 251 (1991).
42. J.M. Courty, S. Reynaud, *Phys. Rev. A* **46**, 2766 (1992).
43. J.-Ph. Poizat, M.J. Collett, D.F. Walls, *Opt. Commun.* **84**, 409 (1991).
44. C.W. Gardiner, *Handbook of Stochastic Methods* (Springer-Verlag, Berlin, 1983); H. Haken, *Laser Theory* (Springer-Verlag, Berlin, 1970).
45. C.W. Gardiner, M.J. Collett, *Phys. Rev. A* **31**, 3761 (1985).
46. M. Lax, *Phys. Rev.* **129**, 2342 (1963); M. Lax, *Phys. Rev.* **157**, 213 (1967); see also P. Meystre, M. Sargent III, *Elements of Quantum Optics*, 2nd edn. (Springer-Verlag, 1990), p. 396; H.J. Carmichael, *An Open Systems Approach to Quantum Optics*, edited by W. Beiglböck (LNIP m18, Springer, 1993).